EUROPEAN ORGANIZATION FOR NUCLEAR RESEARCH

First measurement of Ω_c^0 production in pp collisions at $\sqrt{s} = 13$ TeV

ALICE Collaboration

Abstract

The inclusive production of the charm–strange baryon Ω_c^0 is measured for the first time via its hadronic decay into $\Omega^- \pi^+$ at midrapidity ($|y| < 0.5$) in proton–proton (pp) collisions at the centre-of-mass energy $\sqrt{s} = 13$ TeV with the ALICE detector at the LHC. The transverse momentum (p_T) differential cross section multiplied by the branching ratio is presented in the interval $2 < p_T < 12$ GeV/c. The p_T dependence of the Ω_c^0-baryon production relative to the prompt D^0-meson and to the prompt Ξ_c^0-baryon production is compared to various models that take different hadronisation mechanisms into consideration. In the measured p_T interval, the ratio of the p_T-integrated cross sections of Ω_c^0 and prompt Λ_c^+ baryons multiplied by the $\Omega^- \pi^+$ branching ratio is found to be larger by a factor of about 20 with a significance of about 4σ when compared to e^+e^- collisions.

Recent measurements of charm-baryon production at midrapidity by the ALICE Collaboration [1–5] show that the Λ_c^+/D^0, $\Xi_c^{0,+}/D^0$, and $\Sigma_c^{0,++}/D^0$ baryon-to-meson yield ratios are higher in pp collisions at LHC energies than in e^+e^- collisions, indicating that charm hadronisation occurs via different processes in the two collision systems [6]. The ratios are found to decrease with increasing transverse momentum (p_T), a trend not expected by models based on factorisation and on the usage of the fragmentation functions extracted from e^+e^- collisions. A significant dependence of the p_T-differential Λ_c^+/D^0 ratio with the multiplicity of charged particles produced in the event was also observed in pp collisions at $\sqrt{s} = 13$ TeV [7], possibly suggesting a continuous evolution of this ratio from low-multiplicity pp collisions to the highest multiplicity of charged particles characterising Pb–Pb collisions with a small impact parameter [8].

Higher charm baryon-to-meson ratios in pp collisions with respect to e^+e^- collisions are expected by models that either include dynamical processes that are relevant in quark-and-gluon enriched systems (e.g. colour reconnection beyond leading colour approximation [9] and quark coalescence [10]), or that treat hadronisation as a statistical process [11, 12].

The Lund string fragmentation model [13, 14] implemented in the PYTHIA event generator [15–17], is one of the main hadronisation models used in general-purpose Monte Carlo event generators [18]. In the default version of PYTHIA 8 (Monash 2013 tune [19]), the choice of quarks and gluons that are matched to form strings, encoding colour-confining potentials, is done in the leading-colour approximation. This configuration suppresses the connection of quarks and gluons coming from independent parton scatterings, realising heavy-quark fragmentation and hadronisation schemes very similar to those occurring in e^+e^- collisions. As a result, all of the baryon-to-meson ratios mentioned above are severely underestimated. The extension of colour reconnection beyond the leading colour (CR-BLC) approximation [9] allows the calculations to better approximate quantum chromodynamic colour algebra when matching partons to form strings and enhances the role of "junction" colour-topologies that favour the formation of baryons. The CR-BLC model reproduces the Λ_c^+/D^0 ratio, including the dependence on event multiplicity [7], and the $\Sigma_c^{0,++}/D^0$ ratio [3], but it underestimates the $\Xi_c^{0,+}/D^0$ [4, 5].

In the Catania model [10], charm quarks can hadronise via "vacuum"-like fragmentation as well as recombine (coalesce) with surrounding light quarks from the underlying event. The Wigner formalism is used to calculate the probability to form a baryon (meson) given the phase-space distribution of three (two) quarks. Within uncertainties, this model reproduces the charm baryon-to-meson ratios measured so far in pp collisions, though it tends to systematically underpredict the $\Xi_c^{0,+}/D^0$ and the $\Xi_c^{0,+}/\Sigma_c^{0,++}$ ratios.

In the models implementing hadronisation on a statistical basis, the relative abundances of the various charm-hadron species are determined by statistical weights that depend on the hadron mass, spin, and on the system properties. The p_T dependence of the predicted ratios can have different origins. It derives from the feed-down from higher-mass state decays in the model of Ref. [12], in which a large set of not-yet-observed charm-baryon states is assumed, following the expectation of the relativistic quark model [20]. In the quark-recombination model (QCM) [11] it instead derives from the requirement that charm quarks form hadrons by combining with light quarks with the same velocity. Both models describe the Λ_c^+/D^0 and $\Sigma_c^{0,++}/D^0$ ratios and underestimate the $\Xi_c^{0,+}/D^0$ ratio in pp collisions, with the QCM prediction being closer to the data, although lower by about a factor of two.

The Ω_c^0 baryon is composed of a charm quark and two strange quarks (css). The mentioned models can reproduce Λ_c^+ (cud) data better than $\Xi_c^{0,+}$ (csd, csu) data. This signals a possible difficulty with charm-strange baryons and suggests that the measurement of Ω_c^0 production represents a crucial step to constrain models and understand whether strange quarks, or strange diquarks, play a peculiar role in charm-baryon formation in pp collisions. In high-energy nucleus–nucleus collisions, the production yields of strange hadrons, in particular of multiple-strange baryons, normalised to pion ones are enhanced

with respect to pp collisions and are well described by statistical models using a grand canonical ensemble with strangeness production regulated by chemical equilibrium [21–27]. Measurements of Ω^- and Ξ^- production as a function of the event multiplicity suggest that the onset of such enhancement occurs progressively with increasing particle multiplicity, starting from low-multiplicity pp collisions [25]. In this context, it is however interesting to note that although current data do not exclude that the D_s^+/D^0 ratio in pp collisions could be larger than in e^+e^- collisions, they do not support an increase similar, in relative terms, to that of $\Xi_c^{0,+}/D^0$ ratio. Indeed, the analysis of charm fragmentation fractions reported in Ref. [6] suggests that the branching fraction $c \to \Xi_c^0 + c \to \Xi_c^+$ could be larger than the $c \to D_s^+$ fraction. Another interesting observation is given by the fact that the $\Xi_c^{0,+}/\Sigma_c^{0,++}$ ratio is described well by the default PYTHIA 8 Monash tune [5], which significantly underestimates both $\Xi_c^{0,+}/D^0$ and $\Sigma_c^{0,++}/D^0$ ratios, suggesting that the production of the two baryons could be equally suppressed in e^+e^- collisions because of similar mechanisms. The fraction of Λ_c^+ coming from $\Sigma_c^{0,++}$ decays is larger by a factor of about two in pp collisions than in e^+e^- collisions [3]: this supports the interpretation [9, 28]that in e^+e^- collisions the $\Sigma_c^{0,++}$ formation is suppressed by the need of forming in string breaking a (dd, ud, uu)-diquark with spin $S = 1$, which is heavier than the $S = 0$ (ud)-diquark needed to form a Λ_c^+. A similar argument might be relevant in the comparison of Ω_c^0 and $\Xi_c^{0,+}$ production, possibly influenced by the different mass values of $S = 1$ (ss) and $S = 0$ (sd, su) diquarks [20]. This further highlights the importance of measuring the Ω_c^0 production cross section to understand the role played by strange quarks and diquarks in charm-quark hadronisation. The measurement of the production cross section of the Ω_c^0 baryon is also needed to quantify its possible significant contribution to the total charm cross section at midrapidity per unit of rapidity, both in pp and in Pb–Pb collisions at the LHC [6].

This Letter reports on the first measurement of the p_T-differential production cross section of the inclusive Ω_c^0 baryon multiplied by the branching ratio (BR) of the hadronic decay channel $\Omega_c^0 \to \Omega^-\pi^+$ at midrapidity ($|y| < 0.5$) in pp collisions at $\sqrt{s} = 13$ TeV. Inclusive Ω_c^0 include prompt Ω_c^0, produced directly in the hadronisation of charm quarks or in the decay of directly produced excited charm states, as well as Ω_c^0 from decays of beauty or multiple-charm hadron decays. The ratios of the inclusive Ω_c^0 cross section to the prompt D^0 meson [3] and to the prompt charm–strange Ξ_c^0 baryon [5] are also reported. The absolute branching ratio of the decay channel used has not been measured yet. The Ω_c^0 baryon was reconstructed together with its charge conjugate in the interval $2 < p_T < 12$ GeV/c.

A description of the ALICE detector and its performance can be found in Refs. [29, 30]. The main detectors used for this measurement are the Inner Tracking System (ITS), the Time Projection Chamber (TPC), and the Time-Of-Flight detector (TOF). They are located in the central barrel, which covers the pseudorapidity interval ($|\eta| < 0.9$), and are embedded in a solenoidal magnet that provides a B = 0.5 T field parallel to the beam direction. The ITS is used for tracking, vertex reconstruction, and trigger purposes. The TPC is the main tracking detector in the central barrel and is also used for particle identification (PID) via the measurement of the particle specific energy loss (dE/dx). The TOF provides PID information via the measurement of the particle time-of-flight relative to the time of the collision [31]. The analysed data sample consists of pp collisions at $\sqrt{s} = 13$ TeV recorded with a minimum-bias (MB) trigger based on coincident signals in the two scintillator arrays (V0) located on both sides of the nominal interaction point along the beam direction. Offline selection criteria, based on the signals from the V0 and the Silicon Pixel Detector, which constitutes the two innermost ITS layers, were applied to remove background due to the interaction between one of the beams and the residual gas present in the beam vacuum tube as well as other machine-induced backgrounds [32]. Events with multiple reconstructed primary vertices, which amount to 1% of the total event sample, were rejected to reduce the contamination from the superposition of several collisions within the same colliding bunches (pile-up events). Only events with a primary vertex position within 10 cm from the nominal interaction point along the beam direction were used. After the aforementioned selections, the data sample corresponds to an integrated luminosity $\mathscr{L}_{int} = 32.08 \pm 0.51$ nb^{-1} [33].

The Ω_c^0-baryon candidates were built from $\Omega^- \pi^+$ pairs using a Kalman-Filter (KF) vertexing algorithm [34] by combining a positive charged track (π^+ candidate) originating from the primary vertex and a Ω^--baryon candidate. The Ω^- was reconstructed from the decay chain $\Omega^- \rightarrow \Lambda K^-$, BR $= (67.8 \pm 0.7)\%$, followed by $\Lambda \rightarrow p\pi^-$, BR $= (63.9 \pm 0.5)\%$ [35]. The Ω^- and Λ baryons were reconstructed by exploiting their characteristic decay topologies as reported in Refs. [5, 36]. The tracks of the charged particles involved in the decay chain were required to be in the pseudorapidity interval $|\eta| < 0.8$, to have at least 70 out of 159 crossed TPC tracking points, and to have a fit quality $\chi^2/\text{NDF} < 2$ in the TPC. Moreover, primary π^+ candidates were required to have a minimum of four (out of six) hits in the ITS. Protons, pions, and kaons were selected by requiring compatibility within four standard deviations (4σ) between the measured signal and that expected for the respective particle hypothesis for both the TPC dE/dx and the time-of-flight measurement. Tracks without signal in the TOF detector were identified using only the TPC information. In order to reduce the large combinatorial background, a machine-learning approach based on the adaptive Boosted Decision Tree (BDT) algorithm in the Toolkit for Multivariate Data Analysis (TMVA) [37] was used. The signal sample of Ω_c^0 baryons for the BDT training was obtained from a simulation based on the PYTHIA 8.243 event generator [17]. The mean proper lifetime of Ω_c^0 in the simulation was set to 80 μm according to the latest LHCb measurement [38]. The propagation of the generated particles through the detector was performed using the GEANT 3 package [39]. The luminous region distribution and the conditions of all ALICE detectors in terms of active channels, gain, noise level, and alignment, and their evolution with time during the data taking, were taken into account in the simulations. The background candidates were taken from data by selecting candidates with invariant mass in the intervals $2.39 < M < 2.62$ GeV/c^2 and $2.77 < M < 2.99$ GeV/c^2, which are outside of the expected mass peak of the Ω_c^0. Before the training, loose selections were applied on the distance, normalised to its uncertainty, between the Λ decay point and the primary vertex, and on the Λ, Ω^-, and Ω_c^0 $\chi_{\text{geo}}^2/\text{NDF}$, which is a variable calculated by the KF Particle algorithm [34] related to the intersection probability of the daughter-particle trajectories taking their uncertainties into account. The BDT model was trained independently for each p_T interval with variables related to the Ω^- decay topology, such as the distance of closest approach (DCA) of the decay particles, the DCA between the primary vertex and the reconstructed Ω^- candidate, the pointing angle of the reconstructed Ω^- decay vertex to the reconstructed Ω_c^0 decay vertex, the $\chi_{\text{geo}}^2/\text{NDF}$, and the $\chi_{\text{topo}}^2/\text{NDF}$. The $\chi_{\text{topo}}^2/\text{NDF}$ is calculated by the KF Particle [34] algorithm and characterises whether the Ω^- candidate points back to the reconstructed Ω_c^0 decay vertex. The output of the BDT training allows the classification of each candidate with a number related to its probability to be a Ω_c^0 baryon signal or combinatorial background.

The Ω_c^0 raw yields were obtained from the fit to the invariant-mass distribution of the candidates as shown in the left panel of Fig. 1. The signal peak was modeled with a Gaussian function and the background was described by a linear function.

The p_T and y-differential production cross section in the rapidity interval $|y| < 0.5$ of inclusive Ω_c^0 baryons multiplied by the branching ratio into the considered hadronic decay channel was calculated from the raw yields as follows

$$\text{BR} \times \frac{d^2\sigma^{\Omega_c^0}}{dp_T dy} = \frac{1}{2\Delta y \Delta p_T} \times \frac{N_{\text{raw}}^{\Omega_c^0 + \overline{\Omega}_c^0}}{(\text{Acc} \times \varepsilon)_{\text{inclusive}}} \times \frac{1}{\mathscr{L}_{\text{int}}}, \tag{1}$$

where $N_{\text{raw}}^{\Omega_c^0 + \overline{\Omega}_c^0}$ is the raw yield in a given p_T interval with width Δp_T and in the rapidity interval $\Delta y = 1.6$ assuming that the cross section does not vary significantly from $|y| < 0.5$ to $|y| < 0.8$. To confirm that this assumption has a negligible impact on the result, it was verified that by assuming the rapidity dependence expected for charm mesons in FONLL [40, 41] and for charm baryons in PYTHIA 8 [17] the cross section changes by less than 1% in the measured p_T interval. Since the feed-down contribution is not subtracted, the raw yield is divided by the inclusive acceptance-times-efficiency factor, $(\text{Acc} \times \varepsilon)_{\text{inclusive}}$ and by the

integrated luminosity $\mathscr{L}_{\text{int}}$ of the data sample to obtain the production cross section. The factor $1/2$ is needed to compute the average cross section of Ω_c^0 and $\overline{\Omega}_c^0$. The factor $(\text{Acc} \times \varepsilon)_{\text{inclusive}}$ is the product of the geometrical acceptance (Acc) and the reconstruction and selection efficiency (ε) for the $\Omega_c^0 \to \Omega^- \pi^+$ decay. The $(\text{Acc} \times \varepsilon)_{\text{inclusive}}$ correction was obtained from a simulation with the same configuration as the one used for the BDT training described above. The Ω_c^0-baryon p_{T} distribution from the simulations was reweighted in order to use realistic momentum distributions in the determination of the acceptance and the efficiency, which depends on p_{T}. The weights were defined with an iterative procedure to match the p_{T} dependence measured for Ω_c^0 baryon in the intervals used in the analysis. The right panel of Fig. 1 shows the final $(\text{Acc} \times \varepsilon)$ correction factors of prompt, beauty feed-down, and inclusive Ω_c^0 as a function of p_{T}. They are consistent with each other within uncertainties because the selection variables used are not sensitive to the displacement by a few hundred micrometers of the prompt and beauty feed-down Ω_c^0 decay vertices from the collision point. The efficiency values increase with p_{T} from about 0.7% to about 5%.
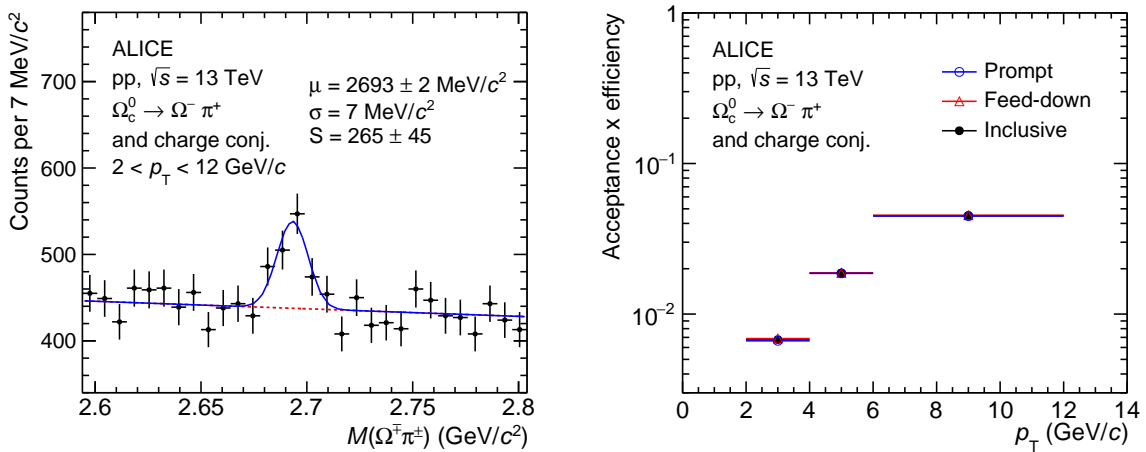

Figure 1: (Left panel): invariant-mass distribution of $\Omega_c^0 \to \Omega^- \pi^+$ candidates and their charge conjugates integrated over the whole p_{T} interval 2–12 GeV/c. The blue line shows the total fit function and the red line represents the combinatorial background fit. (Right panel): acceptance-times-efficiency for prompt, feed-down, and inclusive Ω_c^0 baryons decaying into $\Omega^- \pi^+$ as a function of p_{T} in pp collisions at $\sqrt{s} = 13$ TeV.

Systematic uncertainties were estimated considering several sources. The uncertainty on the track reconstruction efficiency was evaluated by varying the track selection criteria and by comparing the probability to prolong the tracks from the TPC to the ITS hits in data and simulations. A 6% uncertainty was assigned. The systematic uncertainty on the selection efficiency derives from possible differences between the detector resolutions and alignment and their description in the simulation. This uncertainty was assessed from the comparison of the corrected yields obtained by varying the selections. In particular, the selections on the BDT outputs were varied separately in the different p_{T} intervals, with a corresponding variation of the efficiencies ranging from 30% to 50% depending on p_{T}. The assigned systematic uncertainty is 10%, which represents the largest contribution to the systematic uncertainty of the measurement. The systematic uncertainty due to the shape of the Ω_c^0 p_{T} spectrum used in the simulation for the calculation of the $(\text{Acc} \times \varepsilon)_{\text{inclusive}}$ factor was estimated by modifying the weights mentioned above within their uncertainties. An uncertainty of about 4% was estimated in the p_{T} interval $2 < p_{\text{T}} < 4$ GeV/c and a 2% uncertainty in $4 < p_{\text{T}} < 12$ GeV/c. The systematic uncertainty on the raw-yield extraction was evaluated in each p_{T} interval by repeating the fit to the invariant-mass distributions varying the function used to describe the background and the fit range. In order to test the sensitivity to the line-shape of the signal, a bin-counting method was used, in which the signal yield was obtained by integrating the

invariant-mass distribution after subtracting the combinatorial background. A 6% uncertainty was assigned independent of p_T. The sources of systematic uncertainty are assumed to be uncorrelated among each other and the total systematic uncertainty in each p_T interval is calculated by a quadratic sum of the individual contributions, resulting in a 14% systematic uncertainty in $2 < p_T < 4$ GeV/c and 13% in $4 < p_T < 12$ GeV/c. The production cross section has an additional global normalisation uncertainty of 1.6% due to the integrated luminosity determination [33].

The p_T-differential production cross section of inclusive Ω_c^0 baryons multiplied by the branching ratio of the $\Omega^- \pi^+$ channel measured in the rapidity interval $|y| < 0.5$ and the p_T interval $2 < p_T < 12$ GeV/c are shown in Fig. 2. The feed-down contribution from Ω_b^-, e.g. $\Omega_b^- \to \Omega_c^0 + \pi^-$ [35], is not subtracted because of the lack of knowledge of the branching ratios of b-hadron decays to Ω_c^0. Given that the efficiencies of prompt and feed-down Ω_c^0 are consistent within uncertainties, the inclusive measurement presented here preserve the original relative abundances of its prompt and feed-down components. The data are compared with the inclusive Ω_c^0 p_T-differential cross sections expected from the PYTHIA 8.243 Monash and CR-BLC tunes (Mode 2) [9, 17, 19] multiplied by the branching ratio, $BR(\Omega_c^0 \to \Omega^- \pi^+) = (0.51^{+2.19}_{-0.31})\%$, obtained by considering the estimate reported in Ref. [42] for the central value, and the envelope of the values (including their uncertainties) reported in Refs. [42–46] to determine the uncertainty. In the p_T interval of the measurement, the cross section from the CR-BLC tune is larger than the one from the Monash tune by factor varying between 9 and 25 depending on p_T. The Monash tune and CR-BLC tune underestimate the data by more than 3.3σ and 2.7σ, respectively, when $BR(\Omega_c^0 \to \Omega^- \pi^+) = 0.51\%^{+2.19\%}_{-0.31\%}$ is considered.
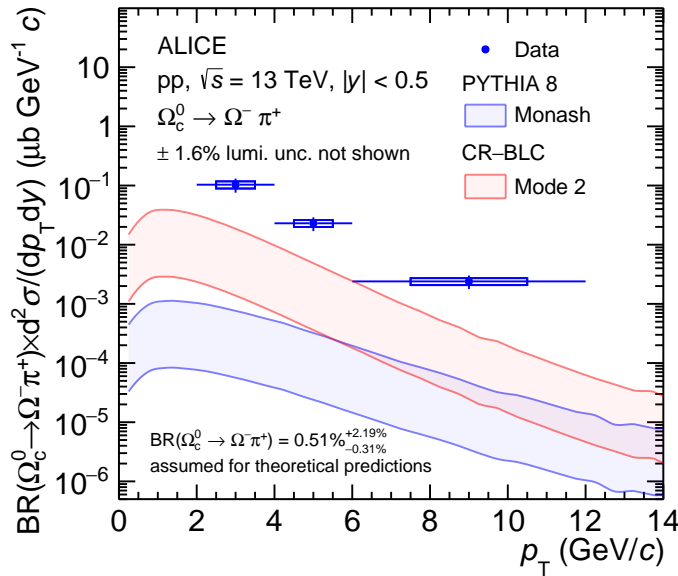

Figure 2: The p_T-differential production cross section of inclusive Ω_c^0 baryons multiplied by the branching ratio into $\Omega^- \pi^+$ for $|y| < 0.5$ in pp collisions at $\sqrt{s} = 13$ TeV. The error bars and empty boxes represent the statistical and systematic uncertainties, respectively. The measurement is compared with PYTHIA 8.243 with Monash tune [19] and with CR beyond the leading-colour approximation [9], which are multiplied by a theoretical $BR(\Omega_c^0 \to \Omega^- \pi^+) = (0.51^{+2.19}_{-0.31})\%$ [42–46].

The ratios of the p_T-differential production cross section of inclusive Ω_c^0 baryons (multiplied by the branching ratio of the $\Omega_c^0 \to \Omega^- \pi^+$ decay channel) to the prompt D^0-meson cross section [3] and to the prompt Ξ_c^0-baryon one [5] are reported in the left and right panel of Fig. 3, respectively. The systematic uncertainties on the tracking efficiency and on the luminosity were propagated as fully correlated in

the ratios. The uncertainties do not allow to draw a conclusion about the possible p_T dependence of the ratios. The data are compared with model expectations that were obtained by scaling the Ω_c^0/D^0 and Ω_c^0/Ξ_c^0 ratios predicted by the models by the BR of the $\Omega_c^0 \to \Omega^- \pi^+$ decay channel mentioned above. The uncertainty band of the models represents the BR uncertainty. For the Catania model only the specific uncertainty of the model itself are also included in the uncertainty band [10]. In the bottom panels, the ratios of the various models and the data to the Catania prediction are shown. The expectations of the models differ significantly, even by orders of magnitude, demonstrating the sensitivity of the measured ratios to the implementation of the charm hadronisation process in the models. As visible in the left panels of Fig. 3, the Monash [19] and CR-BLC [9] tunes of PYTHIA 8, as well as the QCM [11] model underestimate the data significantly. The Monash tune expects a $\mathrm{BR}(\Omega_c^0 \to \Omega^- \pi^+) \times \Omega_c^0/D^0$ ratio increasing with p_T from about 4×10^{-7} to about 1×10^{-5}. The CR-BLC model enhances the ratio by a factor of 12 to 34 with respect to the Monash tune. The prediction of the QCM is larger than that of the CR-BLC model, but it is lower than the data by more than 1.8σ. The Catania model [10] is consistent with the data. In particular, in the version in which additional charm resonance states on top of those listed in the PDG [35] are considered, the Ω_c^0/D^0 ratio is enhanced by a factor of 2, thus enlarging the range of possible $\mathrm{BR}(\Omega_c^0 \to \Omega^- \pi^+)$ values that would allow the model prediction to be compatible within 1σ with the data considering only the data uncertainty. The Ω_c^0/D^0 ratio decreases with p_T in the measured p_T range in the CR-BLC, QCM, and Catania models, oppositely to what is expected by Monash. In the Ω_c^0/Ξ_c^0 baryon-to-baryon ratio, shown in the right panel of Fig. 3, a similar hierarchy among the model predictions is present, though PYTHIA 8 with CR-BLC gives an enhancement by a factor of 4 to 5 with respect to the the Monash expectation, thus smaller than that of the Ω_c^0/D^0 ratio. Also for this ratio, the CR-BLC and QCM predictions are close to each other and higher than the Monash tune. The Catania model shows a good agreement with the data, whether the augmented set of charm resonance states is considered or not.
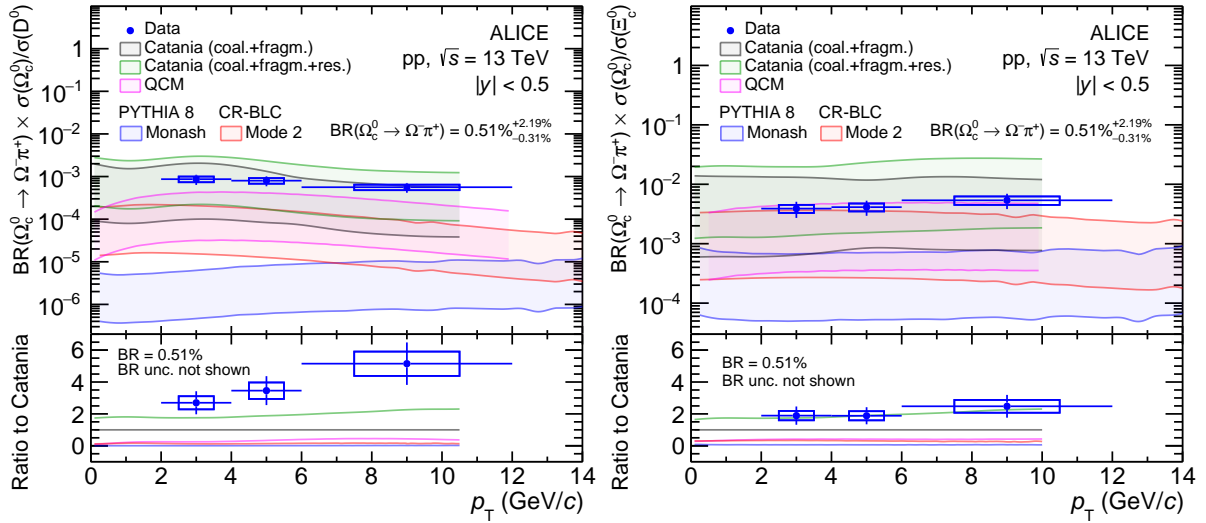

Figure 3: Left, top panel: ratio of the p_T-differential cross section of Ω_c^0 baryons (multiplied by the branching ratio into $\Omega^- \pi^+$) to the D^0-meson one [3] in $|y| < 0.5$ in pp collisions at $\sqrt{s} = 13$ TeV. Right, top panel: ratio of the p_T-differential cross section of Ω_c^0 baryons (multiplied by the branching ratio into $\Omega^- \pi^+$) to the Ξ_c^0-baryon one [5] in $|y| < 0.5$ in pp collisions at $\sqrt{s} = 13$ TeV. Bottom panels: ratio of the data and models to the Catania (coalescence plus fragmentation) model [10]. The error bars and empty boxes represent the statistical and systematic uncertainties, respectively. The measurements are compared with model calculations (see text for details), which are multiplied by a theoretical $\mathrm{BR}(\Omega_c^0 \to \Omega^- \pi^+) = (0.51^{+2.19}_{-0.31})\%$ [42–46].

Using the ALICE Ξ_c^0 [5] and Λ_c^+ [3] data, the ratios $\mathrm{BR}(\Omega_c^0 \to \Omega^- \pi^+) \times \sigma(\Omega_c^0)/\sigma(\Lambda_c^+)$ and $\mathrm{BR}(\Omega_c^0 \to \Omega^- \pi^+) \times \sigma(\Omega_c^0)/\sigma(\Xi_c^0)$ of the cross sections integrated in the Ω_c^0 measured p_T interval were obtained. They are reported in Table 1. They are compared with the values measured in e^+e^- collisions at $\sqrt{s} =$

10.52 GeV by Belle, obtained from the cross sections reported in Table 1 of Ref. [28]. Though the limited p_T and rapidity ranges of the ALICE measurement do not allow for a direct comparison of the pp and e^+e^- data, the ratios observed by ALICE are larger by a factor of 8.7 ± 2.2(stat.)± 0.9(syst.) and 4.7 ± 1.3(stat.)± 0.5(syst.) for the BR($\Omega_c^0 \to \Omega^- \pi^+$) $\times \sigma(\Omega_c^0)/\sigma(\Lambda_c^+)$ and BR($\Omega_c^0 \to \Omega^- \pi^+$) $\times \sigma(\Omega_c^0)/\sigma(\Xi_c^0)$, respectively. The large BR uncertainties of the Ξ_c^0 are not propagated in the computation of this factor. This difference, along with the comparison of data and models in Fig. 3, represents further evidence that the hadronisation process differs in pp and e^+e^- collisions and is sensitive to the density of quarks, colour charges, and on the system size.

Table 1: Ratio of the p_T-integrated cross section of Ω_c^0 baryon (multiplied by the branching ratio into $\Omega^- \pi^+$) in the interval $2 < p_T < 12$ GeV/c with respect to the Λ_c^+- and Ξ_c^0-baryon cross sections measured by the ALICE [3, 5] and Belle [28] experiments in pp collisions at $\sqrt{s} = 13$ TeV and e^+e^- collisions at $\sqrt{s} = 10.52$ GeV, respectively. The first and second uncertainties represent the statistical and systematic ones. The data include the correction for the branching ratio BR($\Omega^- \to \Lambda K^-, \Lambda \to p\pi^-$)=$(43.3 \pm 0.6)\%$ [35].

Ratio	ALICE (pp 13 TeV) $2 < p_T < 12$ GeV/c	Belle (e^+e^- 10.52 GeV) [28] visible
BR($\Omega_c^0 \to \Omega^- \pi^+$) $\times \sigma(\Omega_c^0)/\sigma(\Lambda_c^+)$	$(1.96 \pm 0.42 \pm 0.13) \times 10^{-3}$	$(2.24 \pm 0.29 \pm 0.16) \times 10^{-4}$
BR($\Omega_c^0 \to \Omega^- \pi^+$) $\times \sigma(\Omega_c^0)/\sigma(\Xi_c^0)$	$(3.99 \pm 0.96 \pm 0.96) \times 10^{-3}$	$(8.58 \pm 1.15 \pm 1.98) \times 10^{-4}$

In summary, the inclusive p_T-differential production cross section of the charm-strange baryon Ω_c^0 multiplied by the branching ratio of the $\Omega_c^0 \to \Omega^- \pi^+$ decay channel was measured at midrapidity ($|y| < 0.5$) in pp collisions at $\sqrt{s} = 13$ TeV. The ratio of this measurement to the production cross section of the D^0 meson provides further evidence that charm quarks hadronise to Ω_c^0 baryons more frequently in pp collisions than in e^+e^- collisions, confirming the general trend observed from previous measurements of Λ_c^+, $\Xi_c^{0,+}$, and $\Sigma_c^{0,++}$ production. The large uncertainty of the $\Omega_c^0 \to \Omega^- \pi^+$ branching ratio limits the effectiveness of the comparison with theoretical models. However, the predictions of the available models differ by large factors indicating that future measurements of the BR will allow to exploit these data to set stringent constraints to theoretical models and obtain deep insight into the charm hadronisation and the role of strange quarks and diquarks. Moreover, despite the large uncertainties, only the Catania model, which assumes that charm-quark hadronisation proceeds via both fragmentation and coalescence, can describe the BR($\Omega_c^0 \to \Omega^- \pi^+$) $\times \sigma(\Omega_c^0)/\sigma(D^0)$ ratio within uncertainties. More precise measurements with the data sample collected in Run 3 of the LHC will allow us to further investigate the p_T shape of the Ω_c^0/D^0 and Ω_c^0/Ξ_c^0 ratios.

References

[1] **ALICE** Collaboration, S. Acharya *et al.*, "Λ_c^+ production in pp and in p–Pb collisions at $\sqrt{s_{NN}} = 5.02$ TeV", *Phys. Rev. C* **104** (2021) 054905, `arXiv:2011.06079 [nucl-ex]`.

[2] **ALICE** Collaboration, S. Acharya *et al.*, "Λ_c^+ Production and Baryon-to-Meson Ratios in pp and p–Pb Collisions at $\sqrt{s_{NN}} = 5.02$ TeV at the LHC", *Phys. Rev. Lett.* **127** (2021) 202301, `arXiv:2011.06078 [nucl-ex]`.

[3] **ALICE** Collaboration, S. Acharya *et al.*, "Measurement of Prompt D^0, Λ_c^+, and $\Sigma_c^{0,++}$(2455) Production in Proton–Proton Collisions at $\sqrt{s} = 13$ TeV", *Phys. Rev. Lett.* **128** (2022) 012001, `arXiv:2106.08278 [hep-ex]`.

[4] **ALICE** Collaboration, S. Acharya *et al.*, "Measurement of the production cross section of prompt Ξ_c^0 baryons at midrapidity in pp collisions at $\sqrt{s} = 5.02$ TeV", *JHEP* **10** (2021) 159, `arXiv:2105.05616 [nucl-ex]`.

[5] **ALICE** Collaboration, S. Acharya *et al.*, "Measurement of the Cross Sections of Ξ_c^0 and Ξ_c^+ Baryons and of the Branching-Fraction Ratio $BR(\Xi_c^0 \to \Xi^- e^+ \nu_e)/BR(\Xi_c^0 \to \Xi^- \pi^+)$ in pp collisions at 13 TeV", *Phys. Rev. Lett.* **127** (2021) 272001, `arXiv:2105.05187 [nucl-ex]`.

[6] **ALICE** Collaboration, S. Acharya *et al.*, "Charm-quark fragmentation fractions and production cross section at midrapidity in pp collisions at the LHC", *Phys. Rev. D* **105** (2022) L011103, `arXiv:2105.06335 [nucl-ex]`.

[7] **ALICE** Collaboration, S. Acharya *et al.*, "Observation of a multiplicity dependence in the p_T-differential charm baryon-to-meson ratios in proton–proton collisions at $\sqrt{s} = 13$ TeV", *Phys. Lett. B* **829** (2022) 137065, `arXiv:2111.11948 [nucl-ex]`.

[8] **ALICE** Collaboration, S. Acharya *et al.*, "Constraining hadronization mechanisms with Λ_c^+/D^0 production ratios in Pb–Pb collisions at $\sqrt{s_{NN}} = 5.02$ TeV", `arXiv:2112.08156 [nucl-ex]`.

[9] J. R. Christiansen and P. Z. Skands, "String formation beyond leading colour", *JHEP* **08** (2015) 003, `arXiv:1505.01681 [hep-ph]`.

[10] V. Minissale, S. Plumari, and V. Greco, "Charm hadrons in pp collisions at LHC energy within a coalescence plus fragmentation approach", *Phys. Lett. B* **821** (2021) 136622, `arXiv:2012.12001 [hep-ph]`.

[11] J. Song, H.-h. Li, and F.-l. Shao, "New feature of low p_T charm quark hadronization in pp collisions at $\sqrt{s} = 7$ TeV", *Eur. Phys. J. C* **78** (2018) 344, `arXiv:1801.09402 [hep-ph]`.

[12] M. He and R. Rapp, "Charm-baryon production in proton-proton collisions", *Phys. Lett. B* **795** (2019) 117–121, `arXiv:1902.08889 [nucl-th]`.

[13] B. Andersson, G. Gustafson, and B. Soderberg, "A General Model for Jet Fragmentation", *Z. Phys. C* **20** (1983) 317.

[14] B. Andersson, *The Lund model*, vol. 7. Cambridge University Press, 7, 2005.

[15] T. Sjöstrand, S. Mrenna, and P. Z. Skands, "PYTHIA 6.4 Physics and Manual", *JHEP* **05** (2006) 026, `arXiv:hep-ph/0603175`.

[16] T. Sjöstrand, S. Mrenna, and P. Z. Skands, "A Brief Introduction to PYTHIA 8.1", *Comput. Phys. Commun.* **178** (2008) 852–867, `arXiv:0710.3820 [hep-ph]`.

[17] T. Sjöstrand, S. Ask, J. R. Christiansen, R. Corke, N. Desai, P. Ilten, S. Mrenna, S. Prestel, C. O. Rasmussen, and P. Z. Skands, "An introduction to PYTHIA 8.2", *Comput. Phys. Commun.* **191** (2015) 159–177, `arXiv:1410.3012 [hep-ph]`.

[18] A. Buckley *et al.*, "General-purpose event generators for LHC physics", *Phys. Rept.* **504** (2011) 145–233, `arXiv:1101.2599 [hep-ph]`.

[19] P. Skands, S. Carrazza, and J. Rojo, "Tuning PYTHIA 8.1: the Monash 2013 Tune", *Eur. Phys. J. C* **74** (2014) 3024, `arXiv:1404.5630 [hep-ph]`.

[20] D. Ebert, R. N. Faustov, and V. O. Galkin, "Spectroscopy and Regge trajectories of heavy baryons in the relativistic quark-diquark picture", *Phys. Rev. D* **84** (2011) 014025, `arXiv:1105.0583 [hep-ph]`.

[21] J. Rafelski and B. Muller, "Strangeness Production in the Quark - Gluon Plasma", *Phys. Rev. Lett.* **48** (1982) 1066. [Erratum: Phys.Rev.Lett. 56, 2334 (1986)].

[22] **WA97** Collaboration, E. Andersen *et al.*, "Strangeness enhancement at mid-rapidity in Pb–Pb collisions at 158 A GeV/c", *Phys. Lett. B* **449** (1999) 401–406.

[23] **STAR** Collaboration, B. I. Abelev *et al.*, "Enhanced strange baryon production in Au + Au collisions compared to p + p at $\sqrt{s_{NN}} = 200$ GeV", *Phys. Rev. C* **77** (2008) 044908, arXiv:0705.2511 [nucl-ex].

[24] C. Blume and C. Markert, "Strange hadron production in heavy ion collisions from SPS to RHIC", *Prog. Part. Nucl. Phys.* **66** (2011) 834–879, arXiv:1105.2798 [nucl-ex].

[25] **ALICE** Collaboration, J. Adam *et al.*, "Enhanced production of multi-strange hadrons in high-multiplicity proton-proton collisions", *Nature Phys.* **13** (2017) 535–539, arXiv:1606.07424 [nucl-ex].

[26] **ALICE** Collaboration, B. Abelev *et al.*, "Multi-strange baryon production at mid-rapidity in Pb–Pb collisions at $\sqrt{s_{NN}} = 2.76$ TeV", *Phys. Lett. B* **728** (2014) 216–227, arXiv:1307.5543 [nucl-ex]. [Erratum: Phys.Lett.B 734, 409–410 (2014)].

[27] A. Andronic, P. Braun-Munzinger, K. Redlich, and J. Stachel, "Decoding the phase structure of QCD via particle production at high energy", *Nature* **561** no. 7723, (2018) 321–330, arXiv:1710.09425 [nucl-th].

[28] **Belle** Collaboration, M. Niiyama *et al.*, "Production cross sections of hyperons and charmed baryons from e^+e^- annihilation near $\sqrt{s} = 10.52$ GeV", *Phys. Rev. D* **97** (2018) 072005, arXiv:1706.06791 [hep-ex].

[29] **ALICE** Collaboration, K. Aamodt *et al.*, "The ALICE experiment at the CERN LHC", *JINST* **3** (2008) S08002.

[30] **ALICE** Collaboration, B. Abelev *et al.*, "Performance of the ALICE Experiment at the CERN LHC", *Int.J.Mod.Phys.* **A29** (2014) 1430044, arXiv:1402.4476 [nucl-ex].

[31] **ALICE** Collaboration, J. Adam *et al.*, "Determination of the event collision time with the ALICE detector at the LHC", *Eur. Phys. J. Plus* **132** (2017) 99, arXiv:1610.03055 [physics.ins-det].

[32] **ALICE** Collaboration, B. Abelev *et al.*, "Performance of the ALICE Experiment at the CERN LHC", *Int. J. Mod. Phys. A* **29** (2014) 1430044, arXiv:1402.4476 [nucl-ex].

[33] **ALICE** Collaboration, S. Acharya *et al.*, "ALICE 2016-2017-2018 luminosity determination for pp collisions at $\sqrt{s} = 13$ TeV", Tech. Rep. ALICE-PUBLIC-2021-005, CERN, 2021. https://cds.cern.ch/record/2776672.

[34] I. Kisel, I. Kulakov, and M. Zyzak, "Standalone first level event selection package for the CBM experiment", *IEEE Transactions on Nuclear Science* **60** (2013) 3703–3708.

[35] **Particle Data Group** Collaboration, P. A. Zyla *et al.*, "Review of Particle Physics", *PTEP* **2020** (2020) 083C01.

[36] **ALICE** Collaboration, S. Acharya *et al.*, "Multiplicity dependence of (multi-)strange hadron production in proton-proton collisions at $\sqrt{s} = 13$ TeV", *Eur. Phys. J. C* **80** (2020) 167, arXiv:1908.01861 [nucl-ex].

[37] A. Hocker *et al.*, "TMVA - Toolkit for Multivariate Data Analysis", *CERN-OPEN-2007-007* , `arXiv:physics/0703039`.

[38] **LHCb** Collaboration, R. Aaij *et al.*, "Measurement of the Ω_c^0 baryon lifetime", *Phys. Rev. Lett.* **121** (2018) 092003, `arXiv:1807.02024 [hep-ex]`.

[39] R. Brun, F. Bruyant, F. Carminati, S. Giani, M. Maire, A. McPherson, G. Patrick, and L. Urban, *GEANT: Detector Description and Simulation Tool*. CERN Program Library. CERN, Geneva, 1993. `https://cds.cern.ch/record/1082634`.

[40] M. Cacciari, M. Greco, and P. Nason, "The p_T spectrum in heavy flavor hadroproduction", *JHEP* **05** (1998) 007, `arXiv:hep-ph/9803400 [hep-ph]`.

[41] M. Cacciari, S. Frixione, N. Houdeau, M. L. Mangano, P. Nason, and G. Ridolfi, "Theoretical predictions for charm and bottom production at the LHC", *JHEP* **10** (2012) 137, `arXiv:1205.6344 [hep-ph]`.

[42] Y.-K. Hsiao, L. Yang, C.-C. Lih, and S.-Y. Tsai, "Charmed Ω_c weak decays into Ω in the light-front quark model", *Eur. Phys. J. C* **80** (2020) 1066, `arXiv:2009.12752 [hep-ph]`.

[43] T. Gutsche, M. A. Ivanov, J. G. Körner, and V. E. Lyubovitskij, "Nonleptonic two-body decays of single heavy baryons Λ_Q, Ξ_Q, and Ω_Q $(Q = b, c)$ induced by W emission in the covariant confined quark model", *Phys. Rev. D* **98** (2018) 074011, `arXiv:1806.11549 [hep-ph]`.

[44] H.-Y. Cheng, "Nonleptonic weak decays of bottom baryons", *Phys. Rev. D* **56** (1997) 2799–2811, `arXiv:hep-ph/9612223`. [Erratum: Phys.Rev.D 99, 079901 (2019)].

[45] S. Hu, G. Meng, and F. Xu, "Hadronic weak decays of the charmed baryon Ω_c", *Phys. Rev. D* **101** (2020) 094033, `arXiv:2003.04705 [hep-ph]`.

[46] E. Solovieva *et al.*, "Study of Ω_c^0 and Ω_c^{*0} Baryons at Belle", *Phys. Lett. B* **672** (2009) 1–5, `arXiv:0808.3677 [hep-ex]`.